

Enhanced optical guiding of colloidal particles using a supercontinuum light source

P. Fischer^{1,#}, A. E. Carruthers^{1,#}, K. Volke-Sepulveda², E. M. Wright^{1,3}, C.T.A. Brown¹, W. Sibbett¹ and K. Dholakia^{1,3}

¹*SUPA, School of Physics and Astronomy, University of St Andrews, Fife, KY16 9SS, Scotland*

²*Instituto de Física, UNAM, Apdo. Postal 20-364, 01000 Mexico, D.F., Mexico*

³*College of Optical Sciences, University of Arizona, Tucson, AZ 85711, USA*

contributed equally to this work

fischer@phadreus.ch

toni.carruthers@googlemail.com

Abstract: We demonstrate enhanced optical guiding distances for microscopic particles using a supercontinuum light beam. The enhanced spectral bandwidth of the source leads to an elongated focal region. As a result we obtain a significant radial gradient force and axial radiation pressure force over a longer distance when compared to a monochromatic Gaussian beam. The guiding distances of up to 3mm that are observed for micron-sized particles with the supercontinuum beam are approximately twice those observed using continuous wave and femtosecond laser sources when considering beams of equivalent diameter. This guiding scheme is expected to be applicable to colloidal particles, biological cells and cold atom ensembles.

©2006 Optical Society of America

OCIS codes: 140.7010 Trapping; 080.1010 Aberration theory; 260.2030 Dispersion

References and Links

1. A. Ashkin, "Accelerating and trapping of particles by radiation pressure," *Phys. Rev. Lett.* **24**, 156-159 (1970).
2. C. S. Adams, and E. Riis, "Laser cooling and trapping of neutral atoms," *Prog. Quantum Electron.* **21**, 1-79 (1997).
3. F. Benabid, J. C. Knight, and P. S. J. Russell, "Particle levitation and guidance in hollow-core photonic crystal fiber," *Opt. Express* **10**, 1195-1203 (2002).
4. D. J. Odde, and M. J. Renn, "Laser-guided direct writing of living cells," *Biotechnol. Bioeng.* **67**, 312-318 (2000).
5. M. P. MacDonald, G. C. Spalding, and K. Dholakia, "Microfluidic sorting in an optical lattice," *Nature* **426**, 421-424 (2003).
6. L. Paterson, E. Papagiakoumou, G. Milne, V. Garces-Chavez, S. A. Tatarkova, W. Sibbett, F. J. Gunn-Moore, P. E. Bryant, A. C. Riches, and K. Dholakia, "Light-induced cell separation in a tailored optical landscape," *Appl. Phys. Lett.* **87**, 123901 (2005).
7. I. Ricardez-Vargas, P. Rodriguez-Montero, R. Ramos-Garcia, and K. Volke-Sepulveda, "Modulated optical sieve for sorting of polydisperse microparticles," *Appl. Phys. Lett.* **88** 121116 (2006).
8. A. Ashkin, J. M. Dziedzic, J. E. Bjorkholm, and S. Chu, "Observation of a single-beam gradient force optical trap for dielectric particles," *Opt. Lett.* **11**, 288-290 (1986).
9. J. Arlt, K. Dholakia, J. Soneson, and E. M. Wright, "Optical dipole traps and atomic waveguides based on Bessel light beams," *Phys. Rev. A* **63**, 063602 (2001).
10. A. E. Carruthers, S. A. Tatarkova, V. Garces-Chavez, K. Volke-Sepulveda, S. Chavez-Cerda, and K. Dholakia, "Optical guiding using Gaussian and Bessel light beams," in *Laser Processing of Advanced Materials and Laser Microtechnologies*, F. H. Dausinger, V. I. Konov, V. Y. Baranov, and V. Y. Panchenko, eds. Proc SPIE, **5121**. 68-76 (2003).
11. H. Little, C. T. A. Brown, V. Garces-Chavez, W. Sibbett, and K. Dholakia, "Optical guiding of microscopic particles in femtosecond and continuous wave Bessel light beams," *Opt. Express* **12**, 2560-2565 (2004).
12. R. R. Alfano, and S. L. Shapiro, "Observation of self-phase modulation and small-scale filaments in crystals and glasses," *Phys. Rev. Lett.* **24**, 592-594 (1970).
13. P. Li, K. Shi, and Z. Liu, "Manipulation and spectroscopy of a single particle by use of white-light optical tweezers," *Opt. Lett.* **30**, 156-158 (2005).

14. M. P. MacDonald, L. Paterson, K. Volke-Sepulveda, J. Arlt, W. Sibbett, and K. Dholakia, "Creation and manipulation of three-dimensional optically trapped structures," *Science* **296**, 1101-1103 (2002).
15. G. P. Agrawal, *Nonlinear Fiber optics* (Academic Press, 1995).
16. P. W. Milonni, and J. H. Eberly, *Lasers* (John Wiley & Sons, 1988).
17. R. Gussgard, T. Lindmo, and I. Brevik, "Calculation of the Trapping Force in a Strongly Focused Laser-Beam," *J. Opt. Soc. Am. B* **9**, 1922-1930 (1992).
18. V. Garces-Chavez, K. Volke-Sepulveda, S. Chavez-Cerda, W. Sibbett, and K. Dholakia, "Transfer of orbital angular momentum to an optically trapped low-index particle," *Phys. Rev. A* **66**, 063402 (2002).
19. K. Volke-Sepulveda, S. Chavez-Cerda, V. Garces-Chavez, and K. Dholakia, "Three-dimensional optical forces and transfer of orbital angular momentum from multiringed light beams to spherical microparticles," *J. Opt. Soc. Am. B-Opt. Phys.* **21**, 1749-1757 (2004).
20. L. A. Matheson, and J. L. Saunderson, "Optical and electrical properties of polystyrene," in *Styrene: Its Polymers, Copolymers, and Derivatives*, R. H. Boundy, R. F. Boyer, and S. M. Stoesser, eds. (New York, NY: Reinhold Publishing Co., 1952).
21. P. Fischer, A. E. Carruthers, K. Volke-Sepulveda, E. M. Wright, H. Little, C. T. A. Brown, W. Sibbett, and K. Dholakia, "Enhanced particle guiding using supercontinuum radiation," *Proceedings of the SPIE* (2006).
22. Z. M. Zhu, and T. G. Brown, "Polarization properties of supercontinuum spectra generated in birefringent photonic crystal fibers," *J. Opt. Soc. Am. B-Opt. Phys.* **21**, 249-257 (2004).
23. S. J. Hart, and A. V. Terray, "Refractive-index-driven separation of colloidal polymer particles using optical chromatography," *Appl. Phys. Lett.* **83**, 5316-5318 (2003).

1. Introduction

Optical micro-manipulation remains a very powerful and important technique that has evolved steadily during the three decades since its first demonstration [1]. The forces of light on objects from the size of single atoms right up to the size of a cell have enabled numerous basic and applied scientific procedures that include laser cooling [2], conservative single atom traps based on the dipole force [2], guiding of cells and colloid over large distances for controlled patterning of substrates [3, 4] and optical sorting [5-7]. Optical guiding studies were the precursor for the development of the single beam optical gradient trap known as optical tweezers [8].

Optical guiding has already been realized through the use of both continuous wave [1, 9, 10] and femtosecond [11] laser beams. Optical guiding uses the radial gradient force to localize a particle to the beam axis and the radiation pressure or scattering component of the beam to propel the particle along the axis of the beam. When using a standard Gaussian beam the radial confinement due to the dipole (or gradient) force diminishes rapidly outside the focal region as indeed does the axial radiation pressure force on the particles. Thus the Rayleigh range of the beam is a key component in dictating the maximum guiding distance that may be obtained. Indeed an "ideal" optical guide would have a more uniform radial intensity gradient along its length as well as a uniform axial force. An example that veers in this direction is the Bessel light beam, offering longer guiding distances [11] for cells and colloids due to their propagation invariant nature. However, in such beams, the power is distributed equally amongst a number of surrounding rings. Consequently, the potential depth of the central "non-diffracting" core which constitutes the guide must be traded against the extended guiding distance, thus low guiding velocities are attained in such a scheme. In this paper we demonstrate that bandwidth and dispersion engineering of an ultrashort laser pulse having a Gaussian beam mode profile can be used to generate extended optical guiding with a significantly enhanced guiding distance without having to resort to the use of structured light patterns such as the Bessel light mode. This results in long guiding distances as well as guiding velocities that are comparable with those attained in standard Gaussian guides

It is well known that when focusing with a lens, an elongated focus is created due to chromatic aberration, and the region over which the focus is spread depends on the lens material and the bandwidth of the radiation source used. A laser operating in the femtosecond regime (with a correspondingly extended bandwidth) can thus create a longer focal region compared to a continuous wave (cw) laser. This results in an extended region where we may obtain a strong radial gradient force whilst still obtaining suitable axial radiation pressure for

the guiding. The implication is that for guiding we can engineer a laser beam to have a large radiation bandwidth whilst retaining a suitably high degree of spatial coherence. A femtosecond laser or a supercontinuum (SC) source satisfies these criteria. A supercontinuum source constitutes a very broad bandwidth light source (upwards of 100's of nm) yet retains spatial coherence permitting tight focusing [12]. The inherent chromatic dispersion of the lens allows us to demonstrate elongated guiding distances because different wavelengths are focused at a range of distances beyond the lens. We note that a SC source has been used for tweezing [12] but no study to date has reported any investigations of optical guiding or the exploitation of this elongated focus. (The stacking or alignment of long rods described in reference [13], for example, is not a consequence of the SC beam as it can also result from standard optical tweezing [14] and thus is an inconclusive demonstration of the use of the extended focal extent of such a source.)

2. Modelling

We present numerical models to describe both the propagation of broadband light through our focusing optics and the guiding of microscopic particles in continuous wave, femtosecond and supercontinuum radiation. The first model describes the propagation of radiation with a finite bandwidth through a macroscopic lens and cuvette. Secondly, a ray optics model allows us to calculate both, the axial as well as the transverse forces on microscopic particles in each beam of comparable dimensions.

More specifically, we have compared the guiding distances obtained using a SC beam with the behavior of identical particles with femtosecond and continuous wave laser beams of a similar minimum beam diameter D . We choose the FWHM and power of each of the three beams to be equivalent as it is an accessible experimental parameter and aids direct comparison. We stress optical guiding may also be compared by other means for example by having equivalent guide depth at one position or other valid parameter. There are of course other ways we could define the guide radius, however, we believe our definition as described is as valid as another choice and aids a good comparison between different light sources

Indeed, theoretical modeling of how the bandwidth affects the focal extent of each source and calculations of the axial optical forces provide a physical picture and qualitative support for our experimental findings. Specifically, we can consider an input beam having a power spectrum $S(\lambda)$ and Gaussian spot size w_0 incident on a borosilicate crown glass (BK7) lens of focal length $f(\lambda)$. The wavelength dependent focal length of the lens is given by $f(\lambda)=R/(n(\lambda)-1)$ where R is the radius of curvature, and a Sellmeier formula is used for the refractive index $n(\lambda)$ of the lens material [15]. Beyond the lens at $z=0$, the beam spot size $w(z,\lambda)$ for each wavelength varies with propagation [16] as:

$$w(z,\lambda) = w_0 \sqrt{n_m(\lambda) \left[\left(1 - \frac{1}{f(\lambda)} \left\{ d + \frac{z-d}{n_m(\lambda)} \right\} \right)^2 + \left(\frac{\lambda}{\pi w_0^2} \left\{ d + \frac{z-d}{n_m(\lambda)} \right\} \right)^2 \right]} \quad (1)$$

where d denotes the distance from the lens to the first interface of the cuvette and the particles are suspended in a medium of refractive index $n_m(\lambda)$.

The average intensity profile $I(r,z)$ of the propagating pulse is finally obtained as the sum of the intensity profiles for each wavelength weighted by the power spectrum

$$I(r,z) = \sum_{\lambda} S(\lambda) \cdot I_{\lambda}(r,z) = \sum_{\lambda} S(\lambda) \cdot \frac{2}{\pi w^2(z,\lambda)} \cdot e^{-2\left(r/w(z,\lambda)\right)^2} \quad (2)$$

On the other hand, calculations of the optical forces were realized using a standard ray tracing model [17], which assumes that the incident rays are parallel to the beam axis. In spite of its simplicity, this kind of model has found to give a fairly good qualitative description and in some cases even good quantitative agreement [18, 19] with experimental results for particle

sizes comparable with the wavelength of light thus validating this approach for the data presented here.

Within this approach, the total axial and radial forces can be expressed, respectively, as

$$F_z(r=0, z) = \frac{n_m(\lambda)R_0^2}{2c} P_0 \sum_{\lambda} S(\lambda) \left[\int_0^{\pi/2} \int_0^{2\pi} I_{\lambda}(r_0, z_0) \operatorname{Re}\{Q(\theta, \theta_i; \lambda)\} \sin 2\theta d\varphi d\theta \right], \quad (3)$$

$$F_r(r, z=z_0) = \frac{n_m(\lambda)R_0^2}{2c} P_0 \sum_{\lambda} S(\lambda) \left[\int_0^{\pi/2} \int_0^{2\pi} I_{\lambda}(r_0, z_0) \operatorname{Im}\{Q(\theta, \theta_i; \lambda)\} \sin 2\theta \cos \varphi d\varphi d\theta \right], \quad (4)$$

where,

$$Q(\theta, \theta_i; \lambda) = 1 + R \exp(2i\theta) - T^2 \frac{\exp\{2i(\theta - \theta_i)\} + R \exp(2i\theta)}{1 + R^2 + 2R \cos 2\theta}. \quad (5)$$

Here P_0 is the total power of the beam, R_0 represents the radius of the particle and the integration is carried out over the illuminated hemisphere of the sphere, $0 < \theta < \pi/2$, $0 < \varphi < 2\pi$. The incidence angle coincides with the polar angle θ in this case, and $\theta_i = \theta_t(\lambda)$ is the transmission angle. Each point on the surface of the spherical particle (r_0, z_0) , is related to the position of the particle with respect to the beam axis (r, z) by means of $z_0 = z - R_0 \cos \theta$ and $r_0 = (r^2 + R_0^2 \sin^2 \theta + 2rR_0 \sin \theta \cos \varphi)^{1/2}$. $R = R(\theta, \theta_i, \lambda)$ and $T = T(\theta, \theta_i, \lambda)$ are the reflectance and transmittance Fresnel coefficients, respectively, for the interface between the medium and the particle, averaged over the two orthogonal polarization directions. Notice that the transmission angle and the Fresnel coefficients depend on the wavelength via the refractive indices of the medium and the particle. The refractive index of the polystyrene particles was obtained using the Cauchy dispersion relation [20].

In the experiments performed, the average power is held fixed and equivalent each of the continuous wave, femtosecond, and supercontinuum sources, which means that the normalization $\sum S(\lambda)$ is the same in each case. Table 1 shows the experimentally determined parameters that are also used in the simulations to be presented.

Table 1. Experimental parameters of the light sources: λ_0 is the central wavelength, $\Delta\lambda$ the bandwidth (FWHM), $\Delta\omega/\omega$ the relative bandwidth (1/e), w_0 the Gaussian beam waist before the focusing lens and D the beam diameter (FWHM) at the focus.

	λ_0 [14]	$\Delta\lambda$ (FWHM)	$\Delta\omega/\omega$	w_0 [mm]	D [μm]
Continuous wave laser	780	1	0.001	2.89	11.5
Femtosecond laser	790	100	0.13	3.3	10
Supercontinuum radiation	550	450	0.82	5.02	11

Fig. 1 shows the on-axis intensity $I(0, z)$ versus propagation distance for the cw (blue solid line, $\Delta\lambda/\lambda_0 = 0.001$), femtosecond (green dashed line, $\Delta\lambda/\lambda_0 = 0.13$), and SC (red dotted line, $\Delta\lambda/\lambda_0 = 0.82$) sources, and the inset illustrates the beam profiles $I(r, z_p)$ at the positions $z = z_p$ of peak intensity.

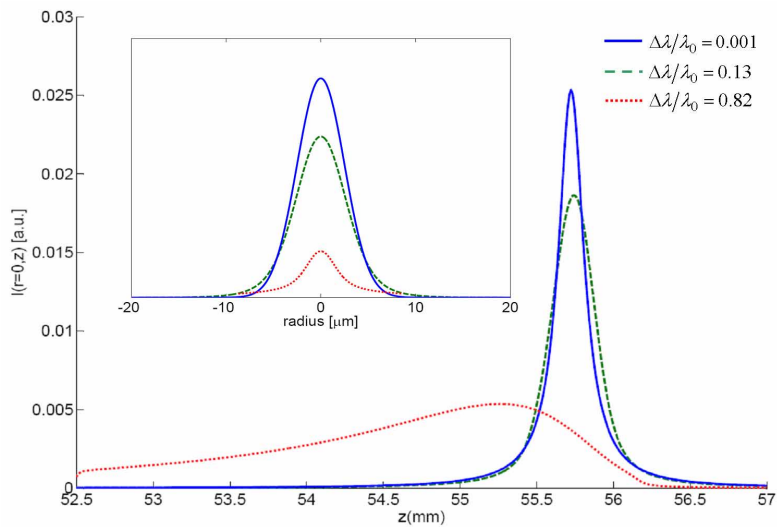


Fig. 1. On-axis intensity distributions $I(0,z)$ and (inset) beam profiles $I(r,z_p)$ of the focused radiation for the continuous wave (solid line), femtosecond (dashed line) Ti:Sapphire laser and the supercontinuum radiation (dotted line). The lens material made of borosilicate crown glass (BK7).

For the cw laser, the spatial extent of the focal region is determined by the Rayleigh range, $z_R = \pi D^2 / 4\lambda_0$, of the focused field (in the case of a fundamental Gaussian beam). However, as the relative bandwidth $\Delta\lambda/\lambda_0$ is increased, dispersion within both the lens and host medium for the particles become more relevant, and its effects are seen both in the decrease of the maximum on-axis intensity and also the elongation of the focal region along the z-axis. It is this elongation of the focus for the supercontinuum source that we propose to enhance the axial spatial extent of the optical guiding.

The intensity profile $I(r,z_p)$ for the continuous wave laser is Gaussian, as shown in the inset in Fig. 1 (blue solid line). As the relative bandwidth $\Delta\lambda/\lambda_0$ is increased the intensity profile is described by the sum of Gaussians in Eq. (2), and the intensity profile develops a broad pedestal as shown in the inset of Fig. 1 for the femtosecond (green dashed line) and SC (red dotted line) sources.

3. Numerical results

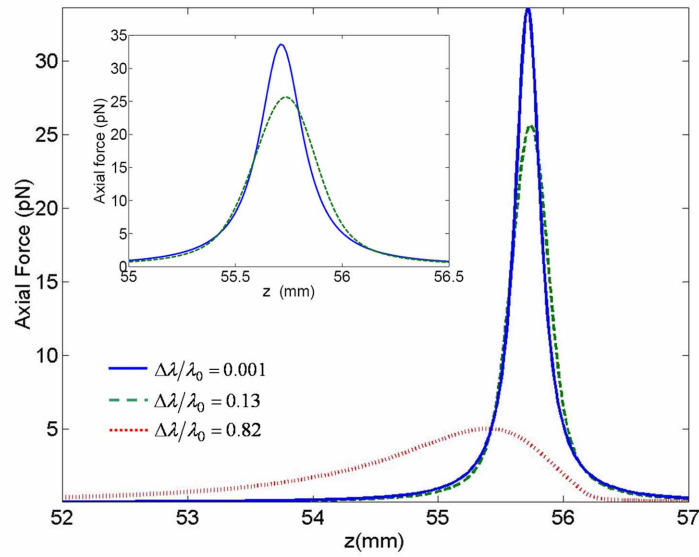
In this section we present numerical results for the forces acting on 5 and 10 microns diameter spheres for the three different sources.

Results for the axial optical force are shown in Fig. 2. When the size of the particle is of the same order or slightly smaller than the minimum beam diameter of the focused beams, the optical force has a very similar behavior to that of the on-axis intensity profile for the three sources. This is verified in Fig. 2(a) for polymer particles of 5 micron diameter.

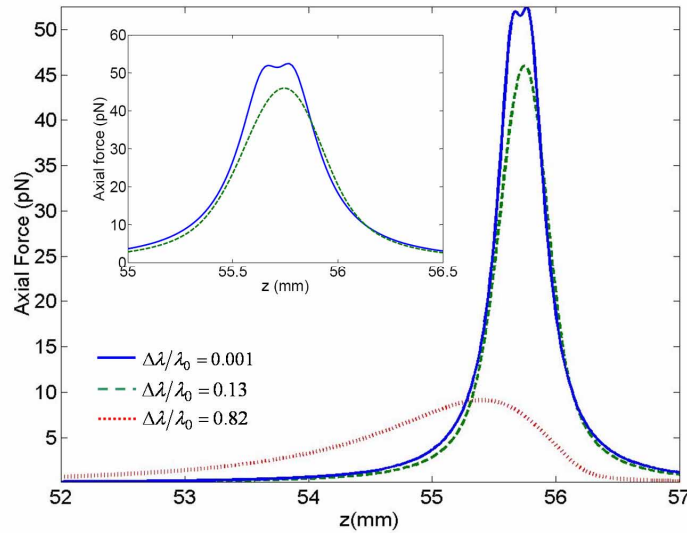
Particles of 1 micron in diameter were guided by the femtosecond and continuous wave beams, however, they were not guided by the supercontinuum beam. As can be seen from Fig. 2, the magnitude of the axial force is much lower for the supercontinuum compared to the femtosecond and continuous wave radiation but extends for a much longer distance. Furthermore, according to our model, optical forces given by Eqs.(3)-(4) also scale with the square of the particle radius. Therefore, both the axial and radial optical forces on the 1 micron particles are, as a first approximation, four times lower than for the 2 micron spheres. This is in agreement with early experimental observations for particles with diameters ranging from 0.6 to 2.7 microns [1], where smaller particles required

higher power levels in order to be guided. However, in this regime, the relative weight of the particles within the host medium is in fact negligible and the thermal effects become more important. Indeed, once the particle goes beyond the focal region thermal and viscous drag forces are enough to pull it out of the guide beam. In that sense, the optical potential well associated to the restoring radial optical force would need to be deep enough to avoid the escape of the particles due to thermal activation or viscous drag. We found radial trapping force to be lower for the supercontinuum than for the other two cases, at the position of minimum beam diameter, but it is sustained over a much longer distance (Fig. 3). This explains why such small particles are not guided but larger particles may indeed be guided readily along the SC beam over an extended distance.

On the other hand, if the particle is larger than the minimum FWHM spot size of the beam, the axial optical force associated with the continuous wave laser exhibits two local maxima at both sides of the beam waist (local minimum), corresponding to the locations where the beam spot is approximately the same as the diameter of the sphere. As a consequence, the continuous wave beam may offer a more extended guiding range than the femtosecond laser in this regime, as is verified in Fig. 2(b) for polymer particles of 10 micron diameter. This behavior becomes more evident as the size of the particle increases for a given beam waist spot, since the local maxima of the axial force would shift outwards for larger particles. Eventually, the axial force for the femtosecond beam will exhibit similar behavior (two local maxima), but this will occur for larger particles since the spot size of this beam is wider than continuous wave beam.



(a)



(b)

Fig. 2. Axial optical force $F(0,z)$ for (a) $5\mu\text{m}$ diameter and (b) $10\mu\text{m}$ diameter polymer spheres for the continuous wave (solid lines), femtosecond (dashed lines) laser and the supercontinuum radiation (dotted lines). Insets show more detailed comparisons for cw and femtosecond lasers.

Figure 3 shows how the transverse or radial restoring force acting on a 5 micron diameter sphere varies with radial displacement r for the three different sources and a variety of marked propagation distances z . Between $z=53\text{--}55\text{mm}$ the radial force for the cw and fs sources are barely discernible compared to the SC source, whereas for $z=56\text{mm}$ the radial forces are comparable. What is clear from this figure is that the radial restoring force for the SC source acts over a longer propagation distance than both the cw and fs sources.

We calculated the radial optical forces for the other particle sizes as well (1, 2 and 10 microns diameters), but found no qualitative differences in the general behavior, in contrast with the case of the axial forces discussed above. We interpret this result in terms of the simple Gaussian-like radial profile of the three sources we are analyzing; important variations in the behavior of the radial forces with particle size have been found only for beams with more structured intensity profiles [19].

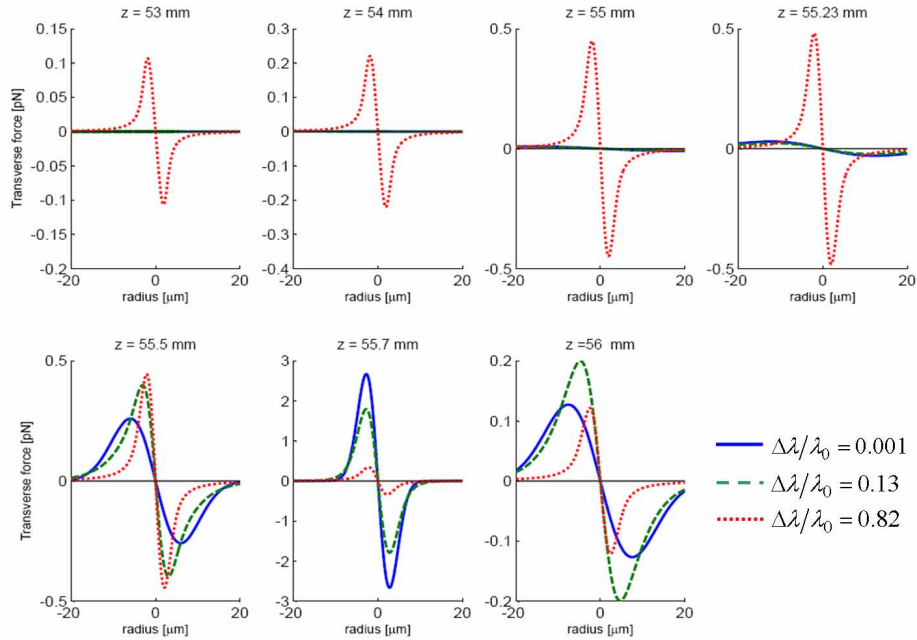


Fig. 3. The radial forces on 5 μ m spheres for the three beams employed in the experiment as a function of radial displacement r for a variety of marked propagation distances z . The colors correspond to cw (blue, solid), fs (green, dashed) and SC (red, dotted). Note how the radial force persists for the SC over a much longer distance than the other beams in turn supporting the notion of a longer guiding distance using this source

Calculations show that a continuous wave Bessel beam of similar dimensions would exert an axial force of 0.36pN on a sphere of 5 microns in diameter, which is more than 13 times lower than the supercontinuum axial force [21].

4. Experimental results

Optical guiding experiments were performed using three optical sources having distinctively different radiation bandwidths, namely, a Ti:Sapphire laser (Femtosome, 780nm 10fs, 80MHz) that could be operated either in a continuous wave non-modelocked or modelocked regimes, and a supercontinuum source. In the modelocked regime the Ti:Sapphire laser resulted in a bandwidth of 100nm (FWHM). The supercontinuum source was generated by propagating pulses from this femtosecond Ti:Sapphire laser through a Femtowhite 800 (Crystal Fibre A/S) polarization-maintaining photonic crystal fiber (PCF) device. We obtained up to 180mW of supercontinuum light with a spectrum ranging from 400nm–1100nm, with a bandwidth of 450nm (FWHM), centered at 550nm.

For a reasonable comparison, the beams were adjusted at focus to be comparable at their FWHM beam diameters D as mentioned earlier (Table 1). The femtosecond and continuous wave beams were resized using a two-lens telescope, $f=50$ mm and 150mm, and the supercontinuum using $f=80$ mm and 500mm. Each guide beam after telescoping was focused

with the same 50mm lens through a high optical quality glass cuvette (of inner dimensions 10mm x10mm x450mm) to create the respective guide beams. The cuvette was kept in the same place, as far as possible, with respect to the focal region of each beam. Particles were observed on a monitor via a charge coupled device with a x20 microscope objective, such that the field of view was approximately 270 μ m.

Polymer particles were used in each respective beam with diameters of 1, 2, 5 and 10 microns (Duke Scientific), and to minimize heating due to medium absorption the particles were immersed in D₂O, due to its lower absorption coefficient than H₂O in the visible and IR regions. For each beam source and particle size, results were recorded for over 50 particles and a standard distribution of guiding distances was obtained. Guiding distances were obtained for each beam with a power of 60mW measured before the final focusing lens.

Particles may enter the beam at any point along the guide. The starting point for determining guiding distances was taken, as far as possible, from particles drifting into the beam from a near on-axis position. This starting point varied by approximately 400 μ m. A more elaborate scheme, could readily allow particles to be loaded into the guide, such that the majority of particles could travel a maximum guiding distance.

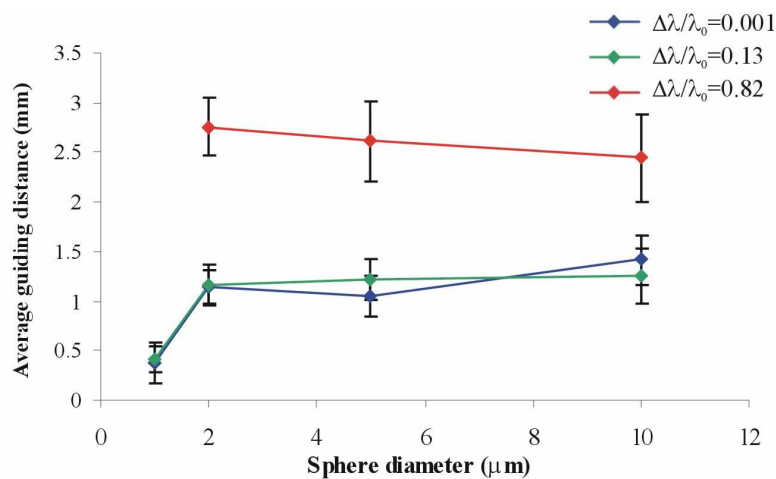


Fig. 4. Optical guiding distances for 1, 2, 5 and 10 micron particles. The 1 micron particles are not guided in the supercontinuum beam for the reasons discussed in the text.

Fig. 4 shows that for 2 micron, 5 micron and 10 micron sphere sizes the supercontinuum source allows particles to be guided further than both the continuous wave and femtosecond beams. Additionally, as expected from the numerical simulations the femtosecond-beam guides slightly further than the continuous wave guide for 2 and 5 micron spheres. More specifically, for 2 micron particles, we found mean guiding distances of 1140 μ m for the continuous wave laser (Standard deviation SD=130 μ m), 1160 μ m for the femtosecond source (SD=100 μ m), and 2760 μ m (SD=190 μ m) for the supercontinuum source, each at a power of 60mW. For the guiding of 5 micron particles we obtained mean guiding distances of 1045 μ m (SD=125 μ m) for the continuous wave source, 1215 μ m (SD=120 μ m) for the femtosecond source, and 2620 μ m (SD=235 μ m) for the SC source at the same average power.

For the 10 micron spheres, however, the continuous wave beam guides slightly further than the femtosecond beam. In particular, the 10 micron spheres guided a mean distance of 2445 μ m for the supercontinuum (SD=265 μ m), compared to 1255 μ m for the femtosecond (SD=155 μ m) and 1415 μ m for the continuous wave beam (SD=180 μ m). This behavior is in agreement with the theoretical findings displayed in Fig. 2(b).

The guiding velocities of 5 micron diameter spheres for supercontinuum, femtosecond and continuous wave beams are shown in Fig. 5. The guiding distance was divided into adjacent regions of approximately 270 μm and the average particle velocities were ascertained through recording the time taken for a particle to cross each field of view. The terminal velocity reached is a balance between the Stokes drag and the axial force in this highly overdamped situation. Guided particles within all beams have near equivalent maximum terminal velocities but as we can see the variation in velocity is higher for the cw and fs beams as expected from the much larger variation in the axial force as a function of distance along the guide. Although some recent work has commented on polarization fluctuations within supercontinuum radiation [22], we have experimentally verified that this has no adverse effect on our system.

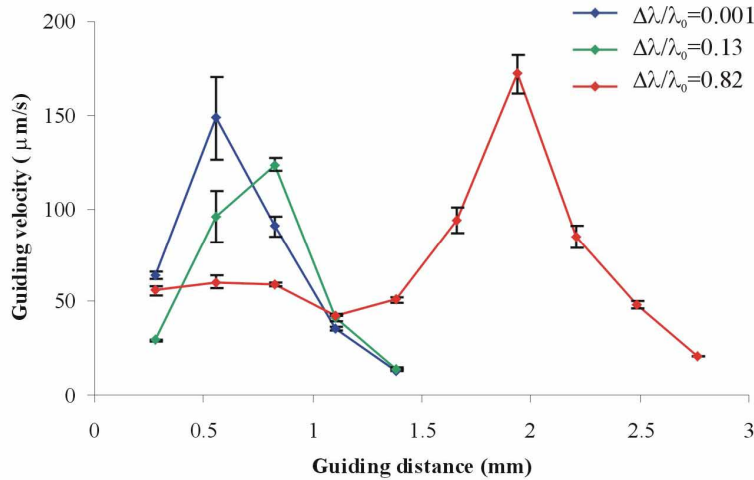


Fig. 5. The variation of average guiding velocity through the optical guide is shown for 5 micron spheres in a supercontinuum, femtosecond and continuous wave beam, each taken at 50mW. The line is given as a guide to the eye. Similar curves have been found for the guiding velocities of 2 micron spheres.

For the case of the supercontinuum guiding the scattered light from the guided particle changes color as it moves through the focal region from deep blue to dark red. This scattering mirrors the spectral component of the beam at the particular axial point in space the particle is traversing. Fig. 6 shows this spectral scattering of light from non-fluorescent 5 micron polymer particles over a guiding distance of 2.94mm. Note that the infrared radiation focused after 2.6mm leads to some heating of the D₂O which causes the spheres to be raised in position due to convection.

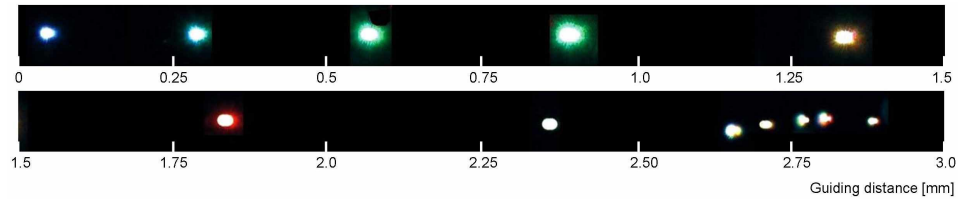


Fig. 6. 5 micron particles are shown over a distance of 2.94mm, guided in a supercontinuum. The scattered light from the guided particle changes color as it moves through the focal region from deep blue to dark red. Note the heating effect of the infrared in the region around 2.75mm which lifts the particle due to convective heating out of the guide.

5. Conclusion

In conclusion, we have demonstrated enhanced guiding distances using a supercontinuum source and we have compared these data to femtosecond and continuous wave beams of similar minimum beam dimensions. In addition, our numerical calculations for the beam propagation characteristics as well as the axial and radial gradients and optical forces support the fact that the radial and axial forces for a SC is sustained over a longer distance compared to a monochromatic cw or femtosecond Gaussian beam, which in turn results in an increased guiding distance. The proposed technique will have applications in long distance cell transport (where one might use a SC source tailored to the near IR 700-1100nm to avoid cell damage), guiding optical droplets and even in cold atom or quantum degenerate gas transport over long distances: indeed, we may create a vortex in any one of these beams that serve to create a suitably long distance hollow guide for cold atoms [9]. Furthermore, the SC beam may also be exploited for enhanced optical chromatography [23] where the radiation pressure from such a guide balances Stokes drag forces for microparticles.

Acknowledgments

We acknowledge Helen Little for initial work on the experiment. The authors would like to acknowledge funding support from the European Science Foundation grant NOMSAN through the SONS Programme through the UK Engineering and Physical Sciences Research Council and the Scottish Higher Education Funding Council through the award of a Strategic Research Development Grant.